with $V_G=10$ V and $V_G=70$ V after the bias heat treatment with a bias voltage of +5 V to the gold layer. At $V_G=70$ V, the photoelectric threshold is less than at $V_G=10$ V and the photoelectric yield at $V_G=70$ V should therefore reveal more structures due to direct transitions than the yield at $V_G=10$ V. However, the structure due to interference is present in both the yields. If the photoelectric yield, i_{70}, at $V_G=70$ V is divided by the photoelectric yield, i_{10}, at $V_G=10$ V, then the resulting curve will be devoid of structures due to interference but will show only structures due to direct transitions. In Fig. 4, we have plotted i_{70}/i_{50} and this curve clearly shows peaks at 3.5, 4.3, and 5.0 eV. In this experiment, we did not observe any distinct peak at 5.7 eV because the terminal state for the 5.7 eV transition was possibly higher than the interface barrier height to start with and, as such, this transition did not increase in strength with band bending. The observation of the peaks at 3.5, 4.3, and 5.0 eV is in good agreement with our results given in Table I.

This experiment has demonstrated that the photoelectric technique in MOS structure is a very convenient tool for studying the energy band diagram of silicon. The attractive feature of this technique lies in the ability to vary the photoelectric threshold gradually by bias heat treatment. However, for this to be possible, the oxide should be fairly contaminated so that there are mobile ions of the order of $10^{12}/cm^2$ or larger. The disadvantage in this method lies in the fact that only degenerate samples will exhibit appreciable shifts in photoelectric threshold. The reason for this is that the distance over which band is bent in silicon is much larger (larger than the optical absorption length and the escape length) for nondegenerate samples than that in degenerate samples.

This method can be extended to the study of the band structure of other semiconductors provided a suitable insulator in MOS geometry can be found. This technique is also convenient for extension to the study of band structure at lower temperatures.

PHYSICAL REVIEW B VOLUME 1, NUMBER 2 15 JANUARY 1970

Room-Temperature Conductivity Anisotropy and Population Redistribution in *n*-Type Silicon at High Electric Fields

P. K. Basu and B. R. Nag
Institute of Radio Physics and Electronics, University of Calcutta, Calcutta, India
(Received 12 March 1969)

Theoretical expressions have been derived for the high-field mobility of carriers in *n*-type Si for any arbitrary direction of field. The distribution function of the electrons in a valley has been assumed to be Maxwellian, and scattering by intravalley acoustic and two types of intervalley phonons have been considered. The conductivity anisotropy for room temperature obtained from theory is of the same order as found experimentally. The population ratio is, however, found to be in disagreement with the values obtained from the analysis of experimental results. A plausible explanation for this disagreement is also presented.

I. INTRODUCTION

EXPERIMENTAL results of high-field conductivity of *n*-type Si at different lattice temperatures are widely reported in the literature.[1–12] A small anisotropy is found in the conductivity characteristics obtained by the conventional methods, at room temperature.[4,11]

A theoretical analysis of the conductivity of *n*-Si at 77°K has been done by Asche and Sarbej[5] and by Asche *et al.*[6] In their analysis the Boltzmann equation was solved by a variational method assuming scattering by acoustic intravalley and two types of intervalley phonons. The characteristic phonon temperatures and coupling constants were taken according to Long.[16] Experimental results for electric field applied along [111] direction were compared with the theory and the agreement was found to be satisfactory. In a later analysis,[6] assuming Maxwellian distribution and including an additional intervalley phonon at 720°K, Asche *et al.* obtained the conductivity characteristics for the [100] direction at 77°K. The calculated characteristics were found to be in agreement with experiment.

[1] E. J. Ryder, Phys. Rev. **90**, 766 (1953).
[2] A. C. Prior, J. Phys. Chem. Solids **12**, 175 (1959).
[3] K. J. Schmidt-Tiedemann, in *Proceedings of the Seventh International Conference on The Physics of Semiconductors, Paris, 1964*, edited by M. Hulin (Academic Press Inc., New York, 1964).
[4] W. E. K. Gibbs, J. Phys. Chem. Solids **25**, 247 (1964).
[5] M. Asche and O. G. Sarbej, Phys. Status Solidi **7**, 339 (1964).
[6] M. Asche, B. L. Boichenko, and O. G. Sarbej, Phys. Status Solidi **9**, 323 (1965).
[7] P. Kastner, E. P. Roth, and K. Seeger, Z. Physik **187**, 359 (1965).
[8] B. L. Boichenko and M. Vasetskii, Fiz. Tverd. Tela **7**, 2021 (1965) [English transl.: Soviet Phys.—Solid State **7**, 1631 (1966).
[9] C. Hamaguchi and Y. Inuishi, J. Phys. Chem. Solids **27**, 1511 (1966).
[10] G. B. Norris and J. F. Gibbons, IEEE Trans. Electron. Devices **ED14**, 38 (1967).
[11] B. R. Nag, H. Paria, and P. K. Basu, Phys. Letters **28A**, 202 (1968).
[12] A. A. Quaranta, M. Martini, G. Ottaviani, G. Redaelli, and G. Zanarini, Solid-State Electron. **11**, 685 (1968).

These authors also studied the dependence of the characteristics on the choice of the coupling constants for the intervalley phonons, but could not find any significant difference for the three sets of values of coupling constants chosen by them.

Recently Costato and Scavo[13,14] assumed a displaced Maxwellian distribution and scattering by acoustic intravalley and a single intervalley phonon with a characteristic temperature quite different from the values given by Long, and they were able to explain the conductivity results of Quaranta *et al.*, who could not detect any anisotropy in the statistical average of the room-temperature data. They have claimed an agreement between theory and experiment over the temperature range from 77° to 300°K. Their calculation, however, is for one field direction, namely the [111] axis.

Duh and Moll,[15] on the contrary, have concluded that Long's two-phonon intervalley scattering and the coupling constants can give excellent fit to their hot-electron–saturated drift-velocity data.

It would appear from the foregoing discussion that the proper theoretical analysis for room-temperature results is yet lacking. The analysis of Costato and Scavo[13,14] for room temperature is based on assumptions quite different from the known scattering mechanisms in n-type Si. In addition, the displaced Maxwellian distribution is likely to occur at very large carrier concentration of the order of $10^{18}/\text{cm}^3$, which is two orders higher than the experimental values.

We present in this paper the conductivity characteristics at room temperature obtained by assuming a Maxwellian distribution and the scattering mechanisms which explain the low-field results. The theoretical derivation is given in Sec. II, and the calculated values are compared with the experimental results in Sec. III.

II. THEORY

The conduction band of silicon is degenerate, with its six valleys situated on ⟨100⟩ axes in the momentum space. The energy of electrons in the jth valley can be expressed as

$$E_j=\tfrac{1}{2}\hbar^2[k_{xj}^2/m_{lj}+k_{yj}^2/m_{tj}+k_{zj}^2/m_{tj}] \qquad (1)$$

in the system of principal axes of the valley under consideration. Here m_l, m_t are, respectively, the longitudinal and transverse effective mass.

When a high electric field F is applied to an n-type Si sample, the distribution of electrons in a valley will depart from its thermal equilibrium value and, in general, will differ from valley to valley. For the jth valley, we expand the distribution function as follows:

$$f_j(\mathbf{k})=f_{0j}(E)+f_{1j}\cos\Theta, \qquad (2)$$

where Θ is the angle between the field and the wave vector. The asymmetric part f_1 is proportional to df_0/dE and to the relaxation time.

The solution for f_{0j} can be obtained from the Boltzmann equation by considering all types of scattering mechanisms. It is well established[16,17] that the important scattering mechanisms in n-type Si at room temperature are acoustic intravalley phonon and intervalley phonon scattering. The effect of the latter can be described by two types of phonons. Among the other scattering mechanisms the impurity scattering and carrier-carrier scattering may be important. At room temperature the effect of impurity scattering is negligible. The carrier-carrier scattering may, however, play an important role in determining the energy and momentum distributions of electrons. For very low electron concentrations, the effect of carrier-carrier scattering may be neglected. For intermediate carrier concentration, this scattering has its effect on the symmetric energy-dependent part only; while for high carrier concentration, this scattering solely determines both the energy and momentum distributions. We assume that the carrier concentration is in the intermediate range, so that the rate of interchange of energy through mutual collision is higher than that arising from the lattice scattering, but the momentum loss by carrier-carrier collision is negligible. With this assumption, the symmetric part of the distribution function becomes Maxwellian[18] and may be expressed as

$$f_{0j}=n_j(\hbar^2/2\pi k_BT_j)^{3/2}(m_{lj}m_{tj}^2)^{-1/2}\exp(-E_j/k_BT_j), \qquad (3)$$

where n_j is the carrier concentration, T_j is the carrier temperature of the jth valley, k_B is the Boltzmann constant, and $\hbar$ is $\frac{1}{2}\pi$ times Planck's constant.

The relaxation time, however, in this case is determined by lattice scattering only and may be calculated as at low fields.

To derive the various terms involved in the Boltzmann equation, we make the usual transformation[19]

$$\mathbf{k}_j^*=(\boldsymbol{\alpha}_j)^{1/2}\cdot\mathbf{k}_j \quad \text{and} \quad \mathbf{F}_j^*=(\boldsymbol{\alpha}_j)^{1/2}\cdot\mathbf{F}, \qquad (4)$$

where $\boldsymbol{\alpha}_j$ is a tensor given by

$$\boldsymbol{\alpha}_j=\begin{bmatrix} \dfrac{m_0}{m_{lj}} & 0 & 0 \\ 0 & \dfrac{m_0}{m_{tj}} & 0 \\ 0 & 0 & \dfrac{m_0}{m_{tj}} \end{bmatrix} \qquad (5)$$

in the system of the principal axes of the valley. We

[13] M. Costato and S. Scavo, Nuovo Ciemento **52B**, 236 (1968).
[14] M. Costato and S. Scavo, Nuovo Ciemento **54B**, 169 (1968).
[15] C. Y. Duh and J. L. Moll, Solid-State Electron. **11**, 917 (1968).
[16] D. Long, Phys. Rev. **120**, 2024 (1960).
[17] J. E. Aubrey, W. Gubler, T. Henningsen, and S. H. Koenig, Phys. Rev. **130**, 1667 (1963).
[18] R. Stratton, Proc. Roy. Soc. (London), **A242**, 355 (1957).
[19] C. Herring and E. Vogt, Phys. Rev. **101**, 944 (1956).

therefore obtain from the Boltzmann equation

$$\left.\frac{\partial f_{0j}}{\partial t}\right|_{\text{field}} = -eF_j^*\frac{1}{3}\left(\frac{2}{m_0}\right)^{1/2} E^{-1/2}\frac{d}{dE}(Ef_{1j}), \tag{6a}$$

$$\left.\frac{\partial f_{0j}}{\partial t}\right|_{\text{lattice}} = \frac{W_{ac0}}{E^{1/2}}\frac{d}{dE}\left[E^2\left(\frac{f_{0j}}{k_BT_L}+\frac{df_{0j}}{dE}\right)\right]$$
$$+\sum_{i=1,2}\frac{W_i}{(k_BT_0)^{3/2}}k_B\theta_i\{\sum_{l\neq j}(E+k_B\theta_i)^{1/2}$$
$$\times[(n_{Li}+1)f_{0l}(E+k_B\theta_i)-n_{Li}f_{0j}(E)]+(E-k_B\theta_i)^{1/2}$$
$$\times[n_{Li}f_{0l}(E-k_B\theta_i)-(n_{Li}+1)f_{0j}(E)]\}, \tag{6b}$$

$$-eF_j^*\left(\frac{2}{m_0}\right)^{1/2}E^{1/2}\frac{df_{0j}}{dE} = -\frac{f_{1j}}{\tau_\lambda}, \tag{6c}$$

where

$$\frac{1}{\tau_\lambda} = \frac{W_{ac\lambda}}{(k_BT_0)^{3/2}}E^{1/2}+\sum_{i=1,2}\frac{W_i}{(k_BT_0)^{3/2}}k_B\theta_i$$
$$\times\sum_{l\neq j}(E+k_B\theta_i)^{1/2}n_{Li}+(E-k_B\theta_i)^{1/2}(n_{Li}+1),$$

$$W_{ac0} = \frac{(2m_0)^{3/2}m_{lj}k_BT_L}{\pi\rho\hbar^4(\det\alpha)^{1/2}}$$
$$\times\tfrac{1}{3}\Xi_u^2[(2+K)r^2+2Kr+K], \tag{6d}$$

$$\frac{W_{ac\lambda}}{(k_BT_0)^{3/2}} = \frac{3}{4}\frac{2^{1/2}m_0^{3/2}k_BT_L\Xi_\lambda^2}{\pi\rho\hbar^4(\det\alpha)^{1/2}u_l^2},$$

$$\Xi_l^2 = \Xi_u^2(1.40r^2+2.40r+1.62),$$

$$\Xi_t^2 = \Xi_u^2(1.33r^2+1.15r+1.07),$$

$$r=\Xi_d/\Xi_u, \quad K=m_l/m_t, \quad n_{Li}=[\exp(\theta_i/T_L)-1]^{-1},$$

m_0 is the free-electron mass, k_B is the Boltzmann constant, T_L is the lattice temperature, T_0 is a normalizing temperature to fix the magnitude of mobility,[16] ρ is the density of the material, and u_l is the velocity of acoustic waves. The equivalent temperatures for the two types of intervalley phonons are 630 and 190°K respectively. The former takes part in the transition from a ⟨100⟩ to the four perpendicular valleys (f scattering), while the latter in the transition from a ⟨100⟩ valley to the opposite ⟨100⟩ valley (g scattering).

To obtain the concentration in different valleys we use the number conservation principle

$$\int\left.\frac{\partial f_j}{\partial t}\right|_{\text{field}}d^3\mathbf{k} = \int\left.\frac{\partial f_j}{\partial t}\right|_{\text{lattice}}d^3\mathbf{k} \tag{7}$$

and obtain from Eqs. (6a) and (6b)

$$n_lT_l^{1/2}[(n_{L1}+1)e^{-\gamma_{1l}}+n_{L1}]I_{1/2}(\gamma_{1l})$$
$$=n_jT_j^{1/2}[(n_{L1}+1)e^{-\gamma_{1j}}+n_{L1}]I_{1/2}(\gamma_{1j}),$$
$$\gamma_{1l}=\theta_1/T_l, \quad \gamma_{1j}=\theta_1/T_j,$$
$$I_{1/2}(x)=\tfrac{1}{2}xe^{1/2x}K_1(\tfrac{1}{2}x). \tag{8}$$

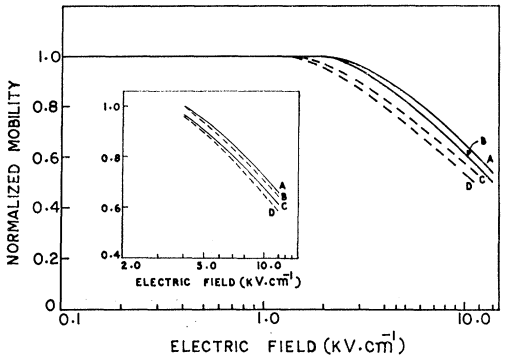

FIG. 1. Mobility at room temperature versus electric field. Curves A and B are theoretical values obtained for electric fields along a ⟨111⟩ and a ⟨100⟩ direction. Curves C and D are the corresponding experimental values obtained by Nag *et al.* Insert: Mobility values normalized by a value corresponding to 4 KV/cm.

K_n is the modified Bessel function of the second kind of order n.

The unknown carrier temperature of the valleys may be obtained from the energy balance condition

$$\int E\left.\frac{\partial f_j}{\partial t}\right|_{\text{field}}d^3\mathbf{k} = \int E\left.\frac{\partial f_j}{\partial t}\right|_{\text{lattice}}d^3\mathbf{k}. \tag{9}$$

Therefore from Eqs. (6a)–(6c) we obtain

$$-n_je^2F_j^{*2}\langle\tau\rangle_j/m_0$$
$$=4W_{ac0}n_j(k_BT_j/\pi)^{1/2}[1-(T_j/T_L)]$$
$$+\sum_{i=1,2}\frac{W_i}{(k_BT_0)^{3/2}}k_B\theta_i\sum_{l\neq j}[2n_l(k_BT_l/\pi)^{1/2}k_BT_l$$
$$\times\{(n_{Li}+1)e^{-\gamma_{il}}I_{3/2,1/2}(\gamma_{il})+n_{Li}I_{1/2,3/2}(\gamma_{il})\}$$
$$-2n_j(k_BT_j/\pi)^{1/2}k_BT_j\{(n_{Li}+1)e^{-\gamma_{ij}}I_{1/2,3/2}(\gamma_{ij})$$
$$+n_{Li}I_{3/2,1/2}(\gamma_{ij})\}], \tag{10}$$

$$\langle\tau\rangle_j = \frac{\int\tau w^{3/2}e^{-w}dw}{\int w^{3/2}e^{-w}dw}. \tag{11}$$

τ is obtained from Eq. (6d).

In these equations we have

$$w=E/k_BT_j, \quad \gamma_{il}=\theta_i/T_l, \quad \gamma_{ij}=\theta_i/T_j,$$

$$I_{m,n}(x_0)=\int_0^\infty x^m(x+x_0)^ne^{-x}dx.$$

Also the mobility is given by

$$\mu = \frac{e}{m_0}\sum_j\frac{n_j}{n}\langle\tau_x\rangle_j\alpha_{xxj}, \tag{12}$$

where n is the total carrier concentration and α_{xxj} is the component of the normalized reciprocal effective mass tensor in the jth valley in the system of the crystal

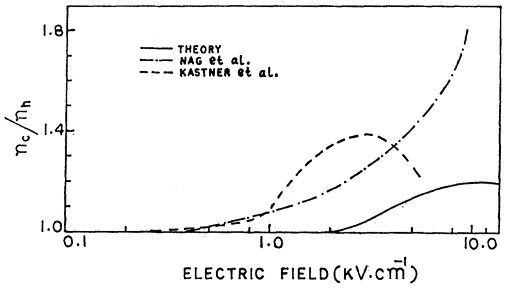

FIG. 2. Ratio of cool to hot valley population (n_c/n_h) for electric field along a ⟨100⟩ direction. Curves obtained by Nag *et al.* and Kastner *et al.* are from the analysis of experimental data.

axes, and $\langle\tau_x\rangle_j$ is the average relaxation time for the x direction.

Using Eqs. (10)–(12) one can find the conductivity and temperature of different valleys for any arbitrary direction of field. We shall, however, restrict our attention to two special cases.

A. Field along the [111] Direction

In this case all the valleys will behave identically and have the same temperature and carrier concentration. We can write, from Eq. (10),

$$\frac{e^2\langle\tau\rangle F^{*2}}{m_0}=4W_{ac0}(k_BT/\pi)^{1/2}[1-(T/T_L)]-\frac{2W_2}{(k_BT_0)^{3/2}}(k_BT/\pi)^{1/2}(k_B\theta_2)^2I_{1/2}(\gamma_2)\times[(n_{L2}+1)e^{-\gamma_2}-n_{L2}]-\frac{8W_1}{(k_BT_0)^{3/2}}(k_BT/\pi)^{1/2}\times(k_B\theta_1)^2I_{1/2}(\gamma_1)[(n_{L1}+1)e^{-\gamma_1}-n_{L1}]. \quad (13)$$

The mobility is

$$\mu_{111}=e[\langle\tau_l\rangle/m_l+2\langle\tau_t\rangle/m_t]. \quad (14)$$

The temperature and mobility for a given field can be obtained from Eqs. (13), (11), and (14).

B. Field along the [100] Direction

In this case the ⟨100⟩ pair of valleys will have temperature lower than that of the remaining four valleys. Denoting cool and hot valleys by the subscript "c" and "h", respectively, one obtains from Eq. (8)

$$n_cT_c^{1/2}[(n_{L1}+1)e^{-\gamma_{1c}}+n_{L1}]I_{1/2}(\gamma_{1c})=n_hT_h^{1/2}[(n_{L1}+1)e^{-\gamma_{1h}}+n_{L1}]I_{1/2}(\gamma_{1h}). \quad (15)$$

For each type of valley an expression is obtained from Eq. (10). The two expressions obtained in the present case can be manipulated to give the following equations:

$$-\frac{e^2\langle\tau\rangle_cF^2}{m_l}\left[1+2\frac{n_h}{n_c}K\frac{\langle\tau\rangle_h}{\langle\tau\rangle_c}\right]=Ac(T_c)+G(T_c)+F_1(T_c)+2\frac{n_h}{n_c}[Ac(T_h)+G(T_h)+F_1(T_h)]=M, \quad (16a)$$

$$-\frac{e^2\langle\tau\rangle_cF^2}{m_l}\left[1-2\frac{n_h}{n_c}K\frac{\langle\tau\rangle_h}{\langle\tau\rangle_c}\right]=Ac(T_c)+G(T_c)+F_2(T_c)-2\frac{n_h}{n_c}[Ac(T_h)+G(T_h)+\tfrac{1}{2}F_1(T_h)+\tfrac{1}{2}F_2(T_h)]=N. \quad (16b)$$

Eliminating F^2 from Eqs. (16a) and (16b), we get

$$\frac{1+2K(n_h/n_c)(\langle\tau\rangle_h/\langle\tau\rangle_c)}{1-2K(n_h/n_c)(\langle\tau\rangle_h/\langle\tau\rangle_c)}=\frac{M}{N}, \quad (16c)$$

where

$$Ac(T_j)=4W_{ac0}(k_BT_j/\pi)^{1/2}[1-(T_j/T_L)],$$

$$G(T_j)=-\frac{2W_2}{(k_BT_0)^{3/2}}(k_B\theta_2)^2(k_BT_j/\pi)^{1/2}I_{1/2}(\gamma_{2j})\times[(n_{L2}+1)e^{-\gamma_{2j}}-n_{L2}],$$

$$F_1(T_j)=-\frac{8W_1}{(k_BT_0)^{3/2}}(k_B\theta_1)^2(k_BT_j/\pi)^{1/2}I_{1/2}(\gamma_{1j})\times[(n_{L1}+1)e^{-\gamma_{1j}}-n_{L1}],$$

$$F_2(T_j)=-\frac{8W_1}{(k_BT_0)^{3/2}}(k_B\theta_1)^2(k_BT_j/\pi)^{1/2}I_{1/2}(\gamma_{1j})\times[(n_{L1}+1)e^{-\gamma_{1j}}+n_{L1}][K_2(\gamma_{1j})/K_1(\gamma_{1j})].$$

The mobility is obtained from the relations

$$\mu_{100}=\frac{2e}{n}\left[\frac{n_c\langle\tau_l\rangle_c}{m_l}+\frac{2n_h\langle\tau_t\rangle_h}{m_t}\right] \quad (17)$$

and

$$n=2n_c+4n_h.$$

III. RESULTS AND DISCUSSION

The conductivity was calculated from the above equations using the following values of the parameters:

$\Xi_u=8.5$ eV, $\Xi_d/\Xi_u=-0.05$, $m_l=0.9m_0$, $m_t=0.192m_0$,

$\rho u_l^2=1.845\times10^{12}$ dyn/cm^2, $\rho=2.33$ g/cm^3,

$W_2/W_{act}=0.15$, $4W_1/W_{act}=2.0$.

The anisotropy in the acoustic relaxation time was neglected and the coupling constant was taken to be equal to the value corresponding to the perpendicular direction. Since the contribution to the mobility from

the parallel component of the mobility tensor is small, the assumption of isotropic relaxation time will not affect the main results. The average over τ was calculated numerically with the aid of a computer for different values of valley temperature.

The calculation of the conductivity for fields along $\langle 111 \rangle$ directions is fairly simple, because all the valleys have equal temperature and population. Inserting an arbitrary value of temperature T in the right-hand side of Eq. (13) and using the corresponding value of $\langle \tau \rangle$ one can solve for the electric field.

To calculate the ratio of population and valley temperatures when the field is along a $\langle 100 \rangle$ direction, it is convenient to assume a value of T_c and different values of T_h. For each pair of values of T_c and T_h the ratio n_h/n_c and $\langle \tau \rangle_h/\langle \tau \rangle_c$ become fixed and can be obtained from Eq. (15) and from the previously calculated values of $\langle \tau \rangle$ at different temperatures. Inserting these values in Eqs. (16a) and (16b) we can calculate the quantities M and N. The procedure is to use different values of T_h for a fixed value of T_c until the ratio M/N equals the ratio in the left-hand side of Eq. (16c). With the values of T_c chosen and of T_h found out, the corresponding field and population ratio can be calculated from Eqs. (16a) and (15), respectively.

The variation of the mobility normalized by their low-field value are illustrated by Fig. 1. Also included in the figure are the experimental values of conductivity for 5-Ω cm n-type Si samples, obtained by Nag *et al.*[11] Results of hot-electron conductivity for samples of different resistivity are available. However, the one we include here for comparison has a concentration of the order of $10^{15}/\text{cm}^3$ and is on the border range of intermediate and high carrier concentration.[18]

The experimental values agree qualitatively with the theory and the anisotropy is of the same order of magnitude. As shown in Fig. 1 when the theoretically and experimentally obtained mobility values are normalized by the respective values for a $\langle 111 \rangle$ direction at a field of 4 KV/cm, at which all the carriers are sufficiently heated, the agreement between theory and experiment becomes more pronounced. It is to be noted that the experimental results quoted by different authors vary by about 30%. Unless the origin of this discrepancy is found out no definite conclusions about the quantitative agreement can be drawn.

The calculated values of the ratio of the cool to hot valley population for different values of fields applied along a $\langle 100 \rangle$ direction are presented in Fig. 2. Kastner *et al.*[7] and Nag *et al.*[11] obtained the population ratio for the same condition from the analysis of the high-field conductivity and Hall mobility results. The values of n_c/n_h obtained by these authors are also shown in Fig. 2 for comparison. We find that the values of present

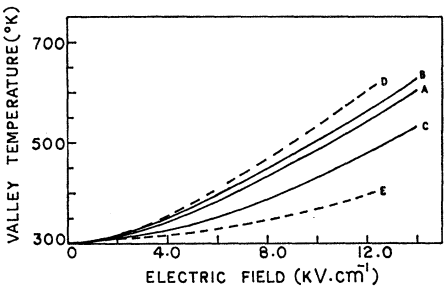

FIG. 3. Valley temperature versus electric field. Curve A gives the temperature for field along a $\langle 111 \rangle$ direction; curves B and C, respectively, the hot and cool valley temperatures for field along a $\langle 100 \rangle$ direction. Curves D and E are the hot and cool valley temperatures obtained from curve A in the effective field approximation (see text).

analysis are much lower than the values obtained from the experimental results. The analyses of the experimental results have been based on the assumption that the mobility of electrons in a valley is solely determined by the effective field in it. However, as is evident from our calculation, the effect of intervalley scattering is quite significant in the energy and momentum exchange processes. Because of the large effect of intervalley scattering, the temperature and the mobility of carriers in a valley will depend also on the conditions in other valleys and cannot be assumed to be solely determined by the effective field in a particular valley. To illustrate this point, we have presented in Fig. 3 the temperature of the valleys for the different directions, obtained from the present analysis. We also show the temperature as obtained by the procedure used in the analysis of experimental results, i.e., by calculating the temperatures of hot and cool valleys, using the results of valley temperature at different fields applied along a $\langle 111 \rangle$ direction. It is evident that the effective field approximation leads to a higher value of temperature for the hot valley and a lower value for the cool valley.

On detailed examination of the results we find that the disagreement between the population ratio obtained in the present analysis and that obtained by Kastner *et al.*[7] and Nag *et al.*[11] may be explained as arising from the above-mentioned assumption in the analysis of experimental results.

ACKNOWLEDGMENTS

The authors are grateful to Professor J. N. Bhar for his kind interest in the work and to Shri D. Mukhopadhyay for helpful discussions. Computer facilities were kindly provided by the Central Instrument Service Section, Indian Institute of Technology, Kharagpur. One of the authors (PKB) expresses his gratitude to the University Grants Commission, India, for the award of a fellowship.